

## The Crystal Structure of Manganese Trifluoride, $\text{MnF}_3$

BY M. A. HEPWORTH AND K. H. JACK

*Chemistry Department, King's College, Newcastle-on-Tyne 1, England*

(Received 4 December 1956)

$\text{MnF}_3$  is monoclinic with  $a = 8.904 \pm 0.003$ ,  $b = 5.037 \pm 0.002$ ,  $c = 13.448 \pm 0.005$  Å;  $\beta = 92.74 \pm 0.04^\circ$ . The structure is pseudo-rhombohedral and has atoms in the following positions of space group  $C2/c-C_{2h}^6$ :

4 Mn at (a): 8 Mn at ( $f_1$ ), with  $x_1 = \frac{1}{2}$ ,  $y_1 = \frac{1}{2}$ ,  $z_1 = \frac{1}{3}$ ; 4 F at (e), with  $y_e = 0.617$ ; 8 F at ( $f_2$ ), with  $x_2 = 0.310$ ,  $y_2 = 0.714$ ,  $z_2 = 0.244$ ; 8 F at ( $f_3$ ), with  $x_3 = 0.167$ ,  $y_3 = 0.117$ ,  $z_3 = 0.583$ ; 8 F at ( $f_4$ ), with  $x_4 = 0.477$ ,  $y_4 = 0.214$ ,  $z_4 = 0.577$ ; 8 F at ( $f_5$ ), with  $x_5 = 0.143$ ,  $y_5 = 0.214$ ,  $z_5 = 0.911$ .

Since its fluorine-atom packing is mid-way between close-packed hexagonal and an  $\text{ReO}_3$ -type cubic close-packing,  $\text{MnF}_3$  is classified as a  $\text{VF}_3$ -type transition-element trifluoride. The lower symmetry of the structure, in comparison with other trifluorides, results from three different Mn-F bond lengths (2.09, 1.91 and 1.79 Å) in each  $\text{MnF}_6$  octahedron. Reasons for this unsymmetrical bonding and for its unique occurrence in  $\text{MnF}_3$  are offered in terms of crystal-field theory.

### Introduction

The classification of transition-element trifluorides into three types according to their fluorine-atom arrangements (Hepworth, Jack, Peacock & Westland, 1957) is correlated with the position of the metal in the Periodic Table. The structure of  $\text{MnF}_3$  was therefore expected to be of the  $\text{VF}_3$ -type. Although this expectation is realized in the present work, it is shown that the distortion of the  $\text{MnF}_6$  octahedra, which are joined by sharing corners, gives rise to a structure of much lower symmetry than that of the other trifluorides in the first long period. The distortion of each  $\text{MnF}_6$  octahedron is due to the occurrence of unequal Mn-F bond lengths, for which an explanation is offered.

### Experimental

$\text{MnF}_3$  was prepared by a modification of the method described by Sharpe & Woolf (1951). Manganous iodate was dissolved in bromine trifluoride and excess of the solvent was evaporated at room temperature under reduced pressure. After heating the solid product in a vacuum at  $140^\circ\text{C}$ ., it was transferred to an alumina boat contained in an alumina tube. Fluorine was passed over it at 20 litres/hour for about 1 hr. at  $500^\circ\text{C}$ . to remove traces of  $\text{BrF}_3$ , to complete the fluorination, and to allow crystal growth. The pale-pink  $\text{MnF}_3$  was transferred to a dry-box and filled into 0.5 mm. diameter X-ray specimen capillaries (found: F 51.3%; calculated for  $\text{MnF}_3$ : F 50.9%).

X-ray photographs were taken at  $18 \pm 2^\circ\text{C}$ . in a 19 cm. Unicam powder camera with crystal-reflected Fe  $K\alpha$  radiation ( $\alpha_1$ , 1.93597;  $\alpha_2$ , 1.93991 Å) from a lithium fluoride monochromator. The relative in-

tensity of each reflexion was measured on at least two films with a Dobson-type microphotometer constructed from a design by Taylor (1951). Since the powder method relies upon the accurate measurement of a limited number of X-ray intensities, special care was taken with the photometry. Exposure times were such that the density of blackening against intensity was kept within the linear portion of the characteristic curve for the emulsion, and, where necessary, differently exposed films, suitably scaled with respect to each other, were used for the measurements of different reflexions. Density readings were taken along the film at 0.01 cm. intervals and the areas under the plotted photometer curves were measured with a planimeter.

### Results

A comparison of the powder photographs of  $\text{FeF}_3$  and  $\text{MnF}_3$  (see Fig. 1) indicated that the structure of the latter was a lower-symmetry distortion of the  $\text{FeF}_3$  rhombohedral structure. By applying various distortions to the  $\text{FeF}_3$  reciprocal lattice, it was concluded that the observed  $\text{MnF}_3$  X-ray reflexions were consistent only with a monoclinic unit cell derived from the orthohexagonal pseudo-cell containing six bimolecular rhombohedral units of a  $\text{VF}_3$ -type structure (see Jack & Gutmann, 1951; Hepworth *et al.*, 1957). Excellent agreement between observed and calculated  $\sin^2 \theta$  values was finally obtained by indexing the  $\text{MnF}_3$  reflexions on the basis of a monoclinic cell with dimensions

$$\begin{aligned} a &= 8.904 \pm 0.003, & b &= 5.037 \pm 0.002, \\ c &= 13.448 \pm 0.005 \text{ Å}; \\ \beta &= 92.74 \pm 0.04^\circ. \end{aligned}$$

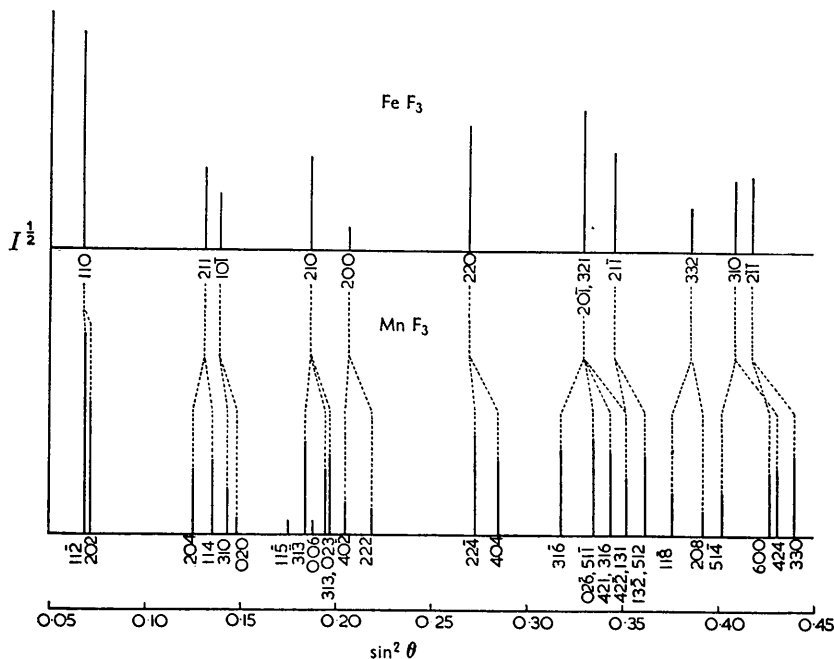


Fig. 1. Comparison of the powder diffraction data of  $\text{FeF}_3$  and  $\text{MnF}_3$ .

For comparison, the orthohexagonal pseudo-cell of iron trifluoride, containing 12  $\text{FeF}_3$ , has dimensions

$$a = \sqrt{3} \cdot b = 9.004, \quad b = 5.198, \quad c = 13.331 \text{ \AA}.$$

The density calculated for 12  $\text{MnF}_3$  per unit cell ( $3.701 \text{ g.cm.}^{-3}$ ) may be compared with the value ( $3.54 \text{ g.cm.}^{-3}$ ) found by Moissan (1900).

The observed absences (see Table 1;  $hkl$  with  $h+k$  odd,  $h0l$  with  $l$  odd,  $0k0$  with  $k$  odd) require space group  $Cc-C_s^4$  or  $C2/c-C_{2h}^6$ ; the structure was provisionally assigned to the centrosymmetrical group  $C2/c$ . In addition, however, there are other systematic absences. The only  $\text{MnF}_3$  reflexions observed have  $2h+l=3n$ . A simple matrix transformation shows that this condition requires a pseudo-rhombohedral symmetry of the structure by which any atom at  $x, y, z$  is related to two identical atoms at  $x+\frac{1}{2}, y+\frac{1}{2}, z+\frac{1}{2}$  and  $x-\frac{1}{2}, y-\frac{1}{2}, z-\frac{1}{2}$ . To satisfy this condition and to preserve correspondence with the metal-atom arrangement in  $\text{FeF}_3$ , twelve manganese atoms were placed in the following positions:

$$4 \text{ Mn at } (a): (0, 0, 0; \frac{1}{2}, \frac{1}{2}, 0) + (0, 0, 0; 0, 0, \frac{1}{2}).$$

$$8 \text{ Mn at } (f_1): (0, 0, 0; \frac{1}{2}, \frac{1}{2}, 0) + \pm(x, y, z; \bar{x}, y, \frac{1}{2}-z),$$

with  $x_1 = 0.167(\frac{1}{6}), y_1 = 0.500(\frac{1}{2}), z_1 = 0.333(\frac{1}{3})$ .

It should be noted that the co-ordinates of the Mn atoms at  $(f_1)$  are related to those at  $(a)$  by  $\pm(\frac{1}{6}, \frac{1}{2}, \frac{1}{3})$ .

The calculated intensity of a powder reflexion ( $hkl$ ) obtained with monochromatic X-radiation and without any temperature correction is given by

$$I_c = \text{constant} \times F_{hkl}^2 \frac{1 + \cos^2 2\alpha \cos^2 2\theta}{\sin^2 \theta \cos \theta} pA, \quad (1)$$

where  $\alpha$  is the angle of reflexion for the monochromator and where the remaining symbols have their usual meanings.

For a structure in which all the atoms vibrate isotropically about their mean lattice positions with equal amplitudes

$$I_o/I_c = \exp \{-2B (\sin \theta/\lambda)^2\} \quad (2)$$

(see Lipson & Cochran, 1953), and, from equations (1) and (2), if

$$\log_{10} I_o - \log_{10} \left\{ F_{hkl}^2 \frac{1 + \cos^2 2\alpha \cos^2 2\theta}{\sin^2 \theta \cos \theta} pA \right\} = \log_{10} Q, \quad (3)$$

then

$$\log_{10} Q = \text{constant} - \frac{2B}{2.303\lambda^2} \sin^2 \theta. \quad (4)$$

Thus, for such a structure, a plot of  $\log_{10} Q$  against  $\sin^2 \theta$  for various reflexions will give a straight line (Bradley & Lu, 1937), from the slope of which the exponential constant ( $B$ ) of the temperature factor may be calculated. It was assumed that the temperature factor for  $\text{MnF}_3$  would be similar to that for  $\text{FeF}_3$  ( $B = 2.24 \text{ \AA}^2$  (Hepworth *et al.*, 1957)). Values of  $\log_{10} Q'$  were first calculated from equation (3) by neglecting any contribution of the fluorine atoms to the structure amplitude, i.e.

$$F' = \sum f_{\text{Mn}} \cos 2\pi(hx + ky + lz) \quad (5)$$

$= 12f_{\text{Mn}}$  for  $l$  even;  $= 0$  for  $l$  odd.

$\log_{10} Q'$  was plotted against  $\sin^2 \theta$  and the deviation of each point (for reflexions with  $l$  even) from a straight line of slope corresponding to  $B = 2.24 \text{ \AA}^2$

then enabled the sign and the approximate magnitude of the fluorine-atom contribution to the structure amplitude to be calculated. Since the contribution of the fluorine atoms is of the same order as that of the manganese atoms for certain reflexions (e.g. 006, 600, 60 $\bar{6}$ , and 0,0,12), the scatter of points representing  $\log_{10} Q'$  was wide. However, by taking into account the maximum possible contribution of the fluorine atoms ( $\pm 36f_F$ ), by adjusting the value of the temperature factor, and by assuming that the fluorine-atom arrangement was not widely different from that of FeF<sub>3</sub>, it was possible to obtain parameters for the fluorine atoms. The procedure was similar to that used in locating the positions of the interstitial atoms in austenite (Petch, 1942; Jack, 1951).

Finally, after trial-and-error refinement, excellent agreement between the observed and calculated X-ray

Table 1. *Calculated and observed X-ray data for MnF<sub>3</sub>*  
(Fe K $\alpha$  radiation)

$$a = 8.904 \pm 0.003, \quad b = 5.037 \pm 0.002, \quad c = 13.448 \pm 0.005 \text{ \AA};$$

$$\beta = 92.74 \pm 0.04^\circ$$

<i>hkl</i>	$\sin^2 \theta$		Relative intensities	
	Calc.	Obs.	Calc.	Obs.
111	0.0548	—	< 1	—
11 $\bar{2}$	0.0681	0.0678	1708	1792
202	0.0712	0.0713	807	800
204	0.1246	0.1246	218	215
114	0.1350	0.1350	260	246
310	0.1437	0.1434	114	108
020	0.1479	0.1481	15	14
11 $\bar{5}$	0.1750	0.1750	8	9
313	0.1837	0.1837	383	395
006	0.1872	0.1881	12	406
023	0.1947	0.1945	193	—
313	0.1973	—	296	496
22 $\bar{1}$	0.1990	0.1974	7	543
40 $\bar{2}$	0.2044	0.2046	45	47
222	0.2191	0.2191	32	31
224	0.2725	0.2725	432	443
404	0.2848	0.2850	223	231
117	0.3089	0.309	5	<i>vw</i>
31 $\bar{6}$	0.3174	0.3176	337	337
225	0.3328	—	1	—
51 $\bar{1}$	0.3348	—	33	—
02 $\bar{6}$	0.3351	0.3351	399	432
316	0.3444	—	287	411
421	0.3457	0.3445	27	315
131	0.3506	—	39	322
42 $\bar{2}$	0.3523	0.3519	121	160
512	0.3617	—	161	157
13 $\bar{2}$	0.3639	0.3624	122	283
11 $\bar{8}$	0.3756	—	80	294
208	0.3922	0.3760	27	79
514	0.4016	0.3921	83	27
600	0.4268	0.4021	183	86
134	0.4308	—	125	—
424	0.4327	0.4314	79	669
330	0.4395	—	278	680
227	0.4396	0.4396	4	—
42 $\bar{5}$	0.4525	—	12	10
13 $\bar{5}$	0.4708	0.4526	37	34
33 $\bar{3}$	0.4795	—	6	—
515	0.4822	0.4821	21	27
333	0.4931	—	3	26
40 $\bar{8}$	0.4984	0.4992	62	65

Table 1 (cont.)

<i>hkl</i>	$\sin^2 \theta$		Relative intensities	
	Calc.	Obs.	Calc.	Obs.
228	0.5401	0.5398	209	271
319	0.5446	0.5448	77	—
2,0,10	0.5526	0.5526	34	32
517	0.5619	0.5620	11	9
029	0.5691	0.5694	36	35
620	0.5747	—	25	—
1,1,10	0.5763	0.5763	114	139
319	0.5852	0.5854	45	148
60 $\bar{6}$	0.5870	—	< 1	86
040	0.5916	0.5917	41	83
137	0.6047	0.6049	10	—
62 $\bar{3}$	0.6080	0.6074	26	58
33 $\bar{6}$	0.6132	—	6	61
427	0.6133	0.6130	16	—
71 $\bar{2}$	0.6282	—	117	—
711	0.6284	0.6294	27	192
53 $\bar{1}$	0.6306	—	48	201
623	0.6350	—	20	—
043	0.6384	0.6397	17	—
336	0.6402	—	9	—
606	0.6410	—	2	—
24 $\bar{1}$	0.6427	—	16	—
42 $\bar{8}$	0.6463	0.6465	86	484
532	0.6575	0.6578	94	495
242	0.6628	0.6628	184	—
1,1,11	0.6697	—	4	—
13 $\bar{8}$	0.6714	0.6715	52	—
518	0.6962	—	47	—
534	0.6974	0.6968	37	109
2,2,10	0.7003	—	25	110
244	0.7160	—	6	—
71 $\bar{5}$	0.7216	—	15	43
714	0.7221	0.7225	22	41
62 $\bar{6}$	0.7349	0.7352	128	—
4,0,10	0.7396	—	3	131
0,0,12	0.7488	0.7488	123	130
245	0.7765	—	19	125
535	0.7780	0.7778	45	—
046	0.7788	—	48	112
626	0.7889	0.7885	92	117
441	0.7894	—	< 1	<i>ms</i>
802	0.7912	0.7912	53	—
44 $\bar{2}$	0.7960	0.7961	108	<i>m</i>
5,1,10	0.8159	—	78	<i>ms</i>
804	0.8176	0.8166	11	—
339	0.8404	—	4	—
2,2,11	0.8410	—	< 1	—
537	0.8577	0.8571	39	<i>mw</i>
3,1,12	0.8655	0.865	19	<i>vw</i>
1,3,10	0.8721	0.8725	40	<i>mw</i>
444	0.8764	0.8765	34	<i>mw</i>
339	0.8810	—	1	—
4,2,10	0.8875	0.8877	102	<i>ms</i>
445	0.8962	—	1	—
0,2,12	0.8967	—	12	—
82 $\bar{1}$	0.9055	—	< 1	—
71 $\bar{8}$	0.9087	—	33	—
717	0.9095	0.9097	40	73
3,1,12	0.9195	0.9193	28	<i>m</i>
732	0.9240	0.9232	25	<i>w</i>
731	0.9242	—	< 1	<i>w</i>
4,2,11	0.9337	—	6	—
1,1,13	0.9374	—	8	—
822	0.9391	—	8	—
151	0.9422	—	7	—
629	0.9554	—	40	—
152	0.9555	0.9561	14	54
1,3,11	0.9655	—	54	<i>w</i>
824	0.9655	0.9668	315	369

data (see Table 1) was obtained by taking  $B=2.43 \text{ \AA}^2$  and by placing 12 Mn and 36 F atoms in the following positions of space group  $C2/c$ :

4 Mn at (a):  $(0, 0, 0; \frac{1}{2}, \frac{1}{2}, 0) + (0, 0, 0; 0, 0, \frac{1}{2})$ .  
 8 Mn at ( $f_1$ ):  $(0, 0, 0; \frac{1}{2}, \frac{1}{2}, 0) + \pm(x, y, z; \bar{x}, y, \frac{1}{2}-z)$ ,  
 with  $x_1 = 0.167(\frac{1}{6})$ ,  $y_1 = 0.500(\frac{1}{2})$ ,  $z_1 = 0.333(\frac{1}{3})$ .  
 4 F at (e):  $(0, 0, 0; \frac{1}{2}, \frac{1}{2}, 0) + \pm(0, y, \frac{1}{4})$ , with  $y_e = 0.617$ .  
 8 F at ( $f_2$ ), with  $x_2 = 0.310$ ,  $y_2 = 0.714$ ,  $z_2 = 0.244$ .  
 8 F at ( $f_3$ ), with  $x_3 = 0.167$ ,  $y_3 = 0.117$ ,  $z_3 = 0.583$ .  
 8 F at ( $f_4$ ), with  $x_4 = 0.477$ ,  $y_4 = 0.214$ ,  $z_4 = 0.577$ .  
 8 F at ( $f_5$ ), with  $x_5 = 0.143$ ,  $y_5 = 0.214$ ,  $z_5 = 0.911$ .

Just as the co-ordinates of the Mn atoms at ( $f_1$ ) are related to those at (a) by  $\pm(\frac{1}{6}, \frac{1}{2}, \frac{1}{3})$ , the F atoms at ( $f_3$ ) are similarly related to those at (e) and the positions ( $f_4$ ) and ( $f_5$ ) are likewise related to ( $f_2$ ).

The estimated error of these atomic co-ordinates is probably not greater than  $\pm 0.003$ . The scattering factors used are those given for the unionized atoms (*International Tables*, 1935) after correction in the case of manganese for dispersion by the  $K$  electrons (see James, 1948; for Fe  $K\alpha$  radiation  $\Delta f_{\text{Mn}} = -4.04$ ). Less satisfactory agreement between the observed and calculated X-ray data was obtained by using scattering-factor values for the fluoride anion; those for the trivalent manganese cation are not available. No evidence was obtained to suggest that the temperature factors of the different atoms in  $\text{MnF}_3$  are unequal or that they are anisotropic.

### Discussion of the $\text{MnF}_3$ structure

Except for the monoclinic distortion of the unit cell, the metal atoms in  $\text{MnF}_3$  are in exactly corresponding positions to those of the  $\text{FeF}_3$  structure. For a similar correspondence between the F-atom arrangements, the values required for the co-ordinates in  $\text{MnF}_3$  would be  $y_e = 0.586$ ;  $x_2 = 0.293$ ,  $y_2 = 0.707$ ,  $z_2 = 0.250$ , with the positions ( $f_3$ ), ( $f_4$ ) and ( $f_5$ ) dependent as before on (e) and ( $f_2$ ). Since the observed co-ordinates are

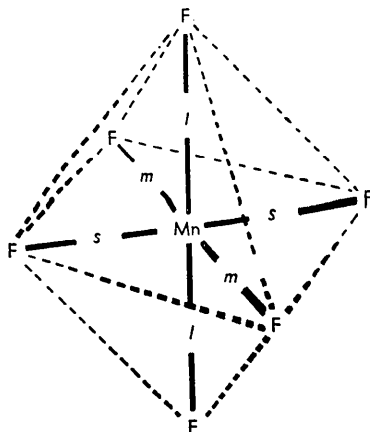


Fig. 2. Dimensions of the  $\text{MnF}_6$  octahedron.

$l = 2.1 \text{ \AA}$ ,  $m = 1.9 \text{ \AA}$ ,  $s = 1.8 \text{ \AA}$ .

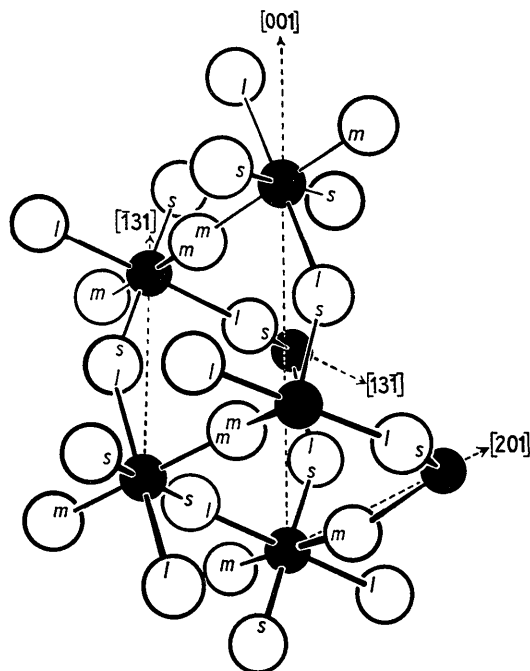


Fig. 3. Spatial relationships between adjacent  $\text{MnF}_6$  octahedra.

appreciably different from these values, it is clear that the fluorine-atom arrangement in  $\text{MnF}_3$  is not merely a small monoclinic distortion of the arrangement in  $\text{FeF}_3$ . The fluorine packing in both trifluorides is approximately mid-way between close-packed hexagonal and a  $\text{ReO}_3$ -type cubic close packing, so that  $\text{MnF}_3$  must be classed like  $\text{FeF}_3$  as a  $\text{VF}_3$ -type transition-element trifluoride. The  $\text{MnF}_3$  structure is, however, much less regular than that of any trifluoride so far reported. It consists of  $\text{MnF}_6$  octahedra joined by sharing all corners. The dimensions of each octahedron are given in Fig. 2, and Fig. 3 shows the relative orientations of neighbouring octahedra. Each Mn is co-ordinated by 6 F: 2 at 2.09, 2 at 1.91 and 2 at 1.79  $\text{\AA}$ . This wide variation in the Mn-F distances within the same octahedral group is unusual. In  $\text{MnF}_2$ , which has the rutile-type structure (Griffel & Stout, 1950), each Mn has 2 F at 2.14 and 4 F at 2.11  $\text{\AA}$ .

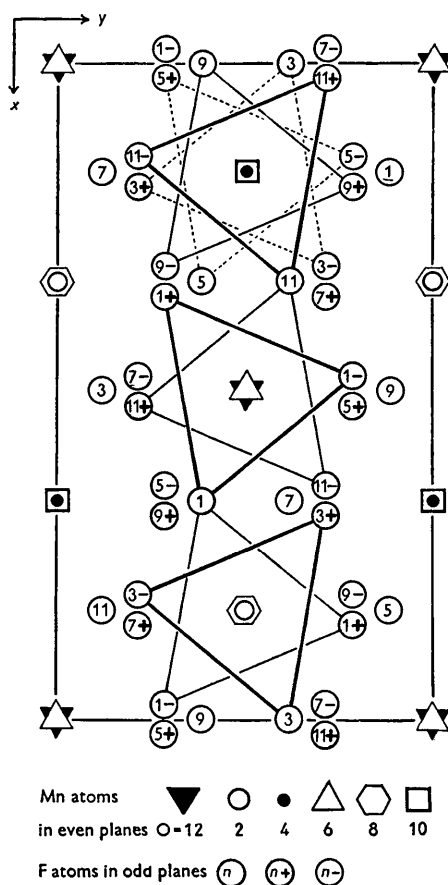
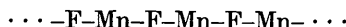
Like  $\text{VF}_3$ , the  $\text{MnF}_3$  structure consists of alternate and regularly spaced planes of metal atoms and planes of fluorine atoms. A projection of the unit cell on (001) along the direction [001] (see Fig. 4) shows twelve such successive planes. Each fluorine-atom plane 1, 3, 5 etc. is puckered and has one-third of its atoms 0.08  $\text{\AA}$  above (+) and one-third 0.08  $\text{\AA}$  below (-) the remaining third. The principal interatomic distances F-F ( $p$  and  $q$ ), M-F ( $r$ ) and M-M ( $s$ ), and the M-F-M bond angles ( $\varphi$ ), are compared with the corresponding distances and angles of  $\text{VF}_3$ ,  $\text{FeF}_3$  and  $\text{CoF}_3$  in Table 2. The mean values for  $\text{MnF}_3$  agree quite closely with those of the related trifluorides, and the individual abnormalities appear to be due to the marked distortion of the  $\text{MnF}_6$  octahedron which results from the

Table 2. Structural data for  $MnF_3$  compared with those for  $VF_3$ ,  $FeF_3$  and  $CoF_3$ 

(Co-ordination numbers are given in parentheses.)

	Interatomic distances (Å)				Bond angle (°)	
	F-F		M-F	M-M		M-F-M
	<i>p</i>	<i>q</i>	<i>r</i>	<i>s</i>		<i>φ</i>
$VF_3$	(4) 2.75	(4) 2.74	(6) 1.94	(6) 3.73	147	
$MnF_3$	(i) { (2) 2.64 (2) 2.81 } 2.73	(2) 2.60 (2) 2.85 } 2.74	(i) (2) 2.09	(i) (2) 3.63 (ii) (4) 3.73 } 3.70	(i) 144	
	(ii) { (2) 2.64 (2) 2.74 } 2.73	(2) 2.60 (2) 2.76 } 2.74	(ii) (2) 1.91		(ii) 148	
	(iii) { (2) 2.74 (2) 2.81 } 2.73	(2) 2.76 (2) 2.85 } 2.74	(iii) (2) 1.79		(iii) 148	
$FeF_3$	(4) 2.72	(4) 2.72	(6) 1.92	(6) 3.73	153	
$CoF_3$	(4) 2.66	(4) 2.69	(6) 1.89	(6) 3.65	149	

three different Mn-F bond lengths. The octahedra are joined by sharing corners in such a way that three sets of linkages

Fig. 4. Projection along [001] on (001) of the  $MnF_3$  unit cell.

run continuously throughout the structure. Since the structure may be regarded as a considerably distorted pseudo-cubic  $ReO_3$  type (Hepworth *et al.*, 1957), the three sets of linkages run in general directions which are approximately at right-angles to one another. The Mn-F distances of the F-Mn-F links in two of these directions are alternately long and short (2.09 and 1.79 Å respectively), and in the third direction the Mn-F distances are all equal (see Fig. 5).

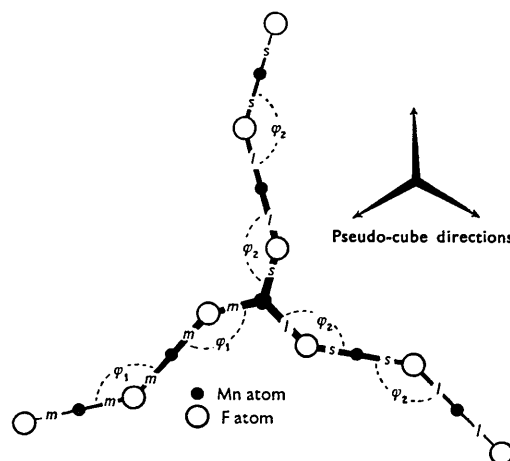


Fig. 5.  
Mn-F bond distances along three pseudo-cubic directions.  
 $l=2.1$  Å,  $m=1.9$  Å,  $s=1.8$  Å;  $\varphi_1=144^\circ$ ,  $\varphi_2=148^\circ$ .

Simple compounds of trivalent manganese are rare, and since no structural data other than those given in the present work are available, values of the Mn-F distance calculated for ionic and for covalent bonding are unreliable. The ionic and covalent radii for fluorine are respectively 1.36 and 0.67 Å, and those for manganese are assessed (see Pauling, 1940; and Sidgwick 1950) as 0.64 and 1.22 Å. Thus, the Mn-F distance is

probably about 2.00 Å for ionic bonding and about 1.89 Å for covalent bonding. The mean of the two shorter observed distances in  $\text{MnF}_3$  (1.91 and 1.79 Å) is slightly less than the estimated covalent value, but the remaining Mn–F bond (2.09 Å) is even longer than the calculated ionic value.

### Interatomic bonding in $\text{MnF}_3$

The crystal-field (or ligand-field) theory (see Orgel, 1952) interprets the stereochemistry of complex compounds of the transition metals by considering the effect of the electric field due to ligand lone-pairs of electrons upon the arrangements of the  $d$ -orbitals of the co-ordinated atom. In the field-free atom (e.g. manganese) the five  $3d$  orbitals are degenerate, but on bringing up six octahedrally co-ordinated charges along the  $x$ ,  $y$  and  $z$  axes a stage is reached when the cubic field is strong enough to split the  $d$ -levels into two groups—a set of three degenerate  $d_e$  orbitals and a set of two  $d_y$  orbitals of higher energy. The  $d_e$  orbitals are of lower energy because their lobes of electron density point in between the  $x$ ,  $y$  and  $z$  axes, i.e. away from the incoming six ligand charges. The  $d_y$  orbitals, however, point along the bond directions, and if they are occupied they will interact repulsively with the incoming charges. As an example of its application, Harris, Nyholm & Stephenson (1956) have recently used the theory to account for the observed bond lengths in  $\text{Pd}(\text{diarsine})_2\text{I}_2$ . The structure of the latter consists of discrete molecules in which the central metal atom is surrounded by 4 As atoms in a square plane at 2.38 Å. The 2 I atoms complete a distorted octahedron with elongated Pd–I bonds (3.52 Å). The normal Pd–I bond distance in square complexes is only 2.65 Å. Prof. R. S. Nyholm (private communication) has suggested that the abnormally long bonds in the  $\text{MnF}_6$  octahedra of the  $\text{MnF}_3$  structure might be explained in a similar way.

The magnetic moment of  $\text{MnF}_3$  is 4.9 B.M. (Nyholm & Sharpe, 1952), from which it is inferred that there are four unpaired electrons in the  $3d$  shell of the Mn(III) atom. Three of these occupy the  $d_e$  orbitals and the remaining electron is most probably in a  $3d_{z^2}$  orbital. The empty  $3d_{(x^2-y^2)}$  orbital points in the directions of four fluorine ions and, together with the  $4s$  and two  $4p$  orbitals, forms four hybrid  $dsp^2$  bonds directed towards the corners of a square. The three singly-occupied  $d_e$  orbitals offer no repulsion since they point between the fluorine atoms. The singly-occupied  $3d_{z^2}$  orbital points along the axis of the remaining two Mn–F bonds and must exert a repulsion. These two F atoms are held either by ionic bonds or by linear hybrid  $4p4d$  bonds—an interpretation which is in accordance with the abnormally long bond length of 2.09 Å. The four hybrid  $3d_{(x^2-y^2)}4s4p^2$  orbitals are not all exactly equivalent since the bonds in the plane (1.91 and 1.79 Å) are not of equal lengths. Neighbouring  $\text{MnF}_6$  octahedra are oriented in such a way that a

fluorine atom common to both is either equidistant at 1.91 Å from each metal atom or is abnormally distant (2.09 Å) from one manganese atom and at the same time abnormally close (1.79 Å) to the other manganese atom. In this way, the close-packing of distorted octahedra with shared corners is maintained. In terms of classical valency theory, the three different Mn–F bonds might be described as having different covalent and ionic contributions, the ionic contribution increasing with increasing bond length.

Ligand-field theory also offers an explanation for the unique difference between manganese and its neighbouring metals in their trifluoride structures. Chromium, manganese, iron and cobalt each in the trivalent state, have electronic configurations represented by:

	$3d_e$			$3d_y$	
Cr	↓	↓	↓		
Mn	↓	↓	↓	↓	
Fe	↓	↓	↓	↓	↓
Co	↓↑	↓	↓	↓	↓

It is only for manganese, where the electron occupation of the  $d_y$  orbitals is unsymmetric, that the  $d_y$  interaction with the ligands might be expected to be anisotropic.

We are greatly indebted to Prof. R. S. Nyholm of University College, London, for most valuable suggestions and for discussion. We also thank Prof. P. L. Robinson of King's College, Newcastle upon Tyne, for his continued interest and encouragement. The work was carried out during the tenure of a British Titan Products Fellowship (M. A. H.), and we acknowledge a grant (to K. H. J.) by the Royal Society for X-ray equipment.

### References

- BRADLEY, A. J. & LU, S. S. (1937). *Z. Kristallogr.* **96**, 20.  
 GRIFFEL, M. & STOUT, J. W. (1950). *J. Amer. Chem. Soc.* **72**, 4351.  
 HARRIS, C. M., NYHOLM, R. S. & STEPHENSON, N. C. (1956). *Nature, Lond.* **177**, 1127.  
 HEPWORTH, M. A., JACK, K. H., PEACOCK, R. D. & WESTLAND, G. J. (1957). *Acta Cryst.* **10**, 63.  
*International Tables for the Determination of Crystal Structures* (1935), vol. 2. Berlin: Borntraeger.  
 JACK, K. H. (1951). *Proc. Roy. Soc. A*, **208**, 200.  
 JACK, K. H. & GUTMANN, V. (1951). *Acta Cryst.* **4**, 246.

- JAMES, R. W. (1948). *The Crystalline State*, vol. 2. London: Bell.
- LIPSON, H. & COCHRAN, W. (1953). *The Crystalline State*, vol. 3. London: Bell.
- MOISSAN, H. (1900). *C. R. Acad. Sci., Paris*, **130**, 662.
- NYHOLM, R. S. & SHARPE, A. G. (1952). *J. Chem. Soc.* p. 3583.
- ORTEL, L. E. (1952). *J. Chem. Soc.* p. 4756.
- PAULING, L. (1940). *The Nature of the Chemical Bond*, 2nd ed. London: Oxford University Press.
- PETCH, N. J. (1942). *J. Iron Steel Inst.* **145**, 111.
- SHARPE, A. G. & WOOLF, A. A. (1951). *J. Chem. Soc.* p. 798.
- SIDGWICK, N. V. (1950). *The Chemical Elements and their Compounds*, vols. 1 and 2. Oxford: Clarendon Press.
- TAYLOR, A. (1951). *J. Sci. Instrum.* **28**, 200.

*Acta Cryst.* (1957). **10**, 351

## A Simple Adapter for Rotation Cameras to Improve the Accuracy of Measurement of Identity Periods

By A. McL. MATHIESON

*Chemical Physics Section, Division of Industrial Chemistry, Commonwealth Scientific and Industrial Research Organization, Melbourne, Australia*

(Received 4 October 1956)

A simple adapter is described which makes it possible to measure identity periods from rotating-crystal photographs with an accuracy of the order of 0.1%.

### Introduction

Identity periods in crystals are related to the separation of layer lines in rotating-crystal photographs by the expression

$$a = n\lambda / \sin \nu_n, \quad (1)$$

where  $a$  is the identity period and  $\nu_n$  the semi-opening cone angle of the  $n$ th layer (Fig. 1). Differentiation of (1) leads to

$$\Delta a/a = -\cot \nu \cdot \Delta \nu, \quad (2)$$

which relates the error in  $a$  to the error in the measurement of  $\nu$ .

For the conventional film mounting in a rotation camera (Fig. 1 (position *A*) and Fig. 2(a)) two factors limit the accuracy. First,  $\nu$  is limited to angles  $< 55^\circ$ , so that  $\cot \nu$  is always  $> 0.7$ . Secondly, in the terminology of Buerger (1942, p. 95),  $\Delta \nu = \cos^2 \nu / r \cdot \Delta y$ , where  $r$  is the radius of the camera and  $\Delta y$  is the error in the measurement of the separation of the layer lines. At the upper limit of  $\nu$ ,  $\cos^2 \nu = 0.3$ , but, owing to beam divergence and oblique incidence of the diffracted beams on the double-coated film,  $\Delta y$  increases about 4–5 times (a value determined from Fig. 2(a), but representative of typical rotation photographs) and hence  $\Delta \nu$  for upper layer lines is slightly greater than for lower layer lines. The expected increase in accuracy for upper layer lines due to the  $\cot \nu$  term in (2) is therefore partly reduced by the increase in  $\Delta \nu$ .

### Principle of the adapter

A film mounting which would permit normal incidence of reflexions in the range  $0^\circ < \nu < 90^\circ$ , would over-

come these disadvantages (Fig. 1 (position *B*)) since the size of reflexions would not vary with  $\nu$  for a small crystal of the usual dimensions.  $\Delta \nu$  would remain constant and full advantage could be taken of the

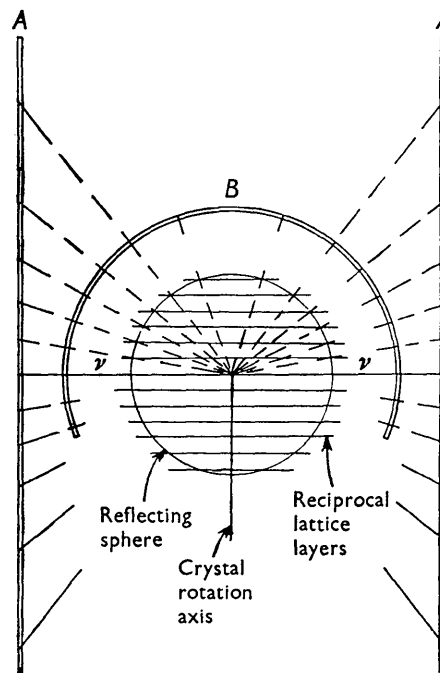


Fig. 1. Rotating-crystal technique with film in the standard position *A* and in the modified position *B* permitting normal incidence of reflexions. The direct X-ray beam is normal to the plane of the paper and the diagram illustrates the section at  $2\theta = 90^\circ$ .